



ELSEVIER

International Journal of Thermal Sciences 41 (2002) 936–948

International  
Journal of  
Thermal  
Sciences

www.elsevier.com/locate/ijts

# Hydromagnetic double-diffusive convection in a rectangular enclosure with uniform side heat and mass fluxes and opposing temperature and concentration gradients

Ali J. Chamkha \*, Hameed Al-Naser

*Department of Mechanical Engineering, Kuwait University, PO Box 5969, Safat 13060, Kuwait*

Received 4 April 2001; accepted 5 November 2001

## Abstract

The problem of hydromagnetic double-diffusive convective flow of a binary gas mixture in a rectangular enclosure with the upper and lower walls being insulated is solved numerically by the finite-difference methodology. Constant heat and mass fluxes conditions are imposed along the left and right walls of the enclosure and a uniform magnetic field is applied in the direction normal to the left and right walls. In this study, the thermal and the compositional buoyancy forces are assumed to be opposite and internal heat generation or absorption effects are assumed to exist. Numerical results illustrating the effects of the heat generation or absorption coefficient and the Hartmann number on the contours of streamline, temperature and concentration are presented graphically. In addition, results for the velocity, temperature and concentration profiles at mid-section of the enclosure as well as the average Nusselt and Sherwood numbers are presented and discussed for various parametric conditions.

© 2002 Éditions scientifiques et médicales Elsevier SAS. All rights reserved.

## 1. Introduction

Double-diffusion natural convection occurs in a wide range of scientific fields such as oceanography, astrophysics, geology, biology, chemical vapor transformation processes, pollution, and crystal growth techniques, such as semi-conductors and alloys, where temperature and concentration differences are combined (see, for instance, [5,7]). Ostrach [22]) and Viskanta et al. [30] reported complete reviews on the subject. Bejan [6] reported a fundamental study of scale analysis relative to heat and mass transfer within cavities submitted to horizontal combined and pure temperature and concentration gradients. Kamotani et al. [14] considered an experimental study of natural convection in shallow enclosures with horizontal temperature and concentration gradients. Other experimental studies dealing with thermo-solutal convection in rectangular enclosures were reported by Ostrach et al. [23] and Lee et al. [16]. Lee and Hyun [17] and Hyun and Lee [12] reported numerical solutions for unsteady double-diffusive convection in a rectangular

enclosure with aiding and opposing temperature and concentration gradients, which were in good agreement with, reported experimental results. Trevisan and Bejan [28] studied combined heat and mass transfer by natural convection in a vertical enclosure having two adiabatic and impermeable horizontal walls and two heat and mass isoflux vertical walls. Alavyoon and Masuda [2] investigated natural convection in vertical enclosures filled with porous media due to opposing fluxes of heat and mass prescribed at the vertical walls.

Electrically conducting fluids in the presence of a magnetic field have been used extensively in many applications such as crystal growth, geothermal reservoir, metallurgical applications involving continuous casting and solidification of metal alloys and others. Oreper and Szekely [21] found that the presence of a magnetic field can suppress natural convection currents and that the strength of the magnetic field is one of the important factors in determining the quality of the crystal. Ozoe and Maruo [24] investigated magnetic and gravitational natural convection of melted silicon two-dimensional numerical computations for the rate of heat transfer. Alchaar et al. [3] considered natural convection heat transfer in a rectangular porous enclosure having two insulated walls and the other two walls are maintained at constant

\* Correspondence and reprints.

*E-mail address:* chamkha@kuc01.kuniv.edu.kw (A.J. Chamkha).

**Nomenclature**

$A$	enclosure aspect ratio = $H/W$	$W$	enclosure width
$B_o$	magnetic induction	$x$	horizontal coordinate
$c$	concentration of species	$X$	dimensionless horizontal coordinate = $x/W$
$c_r$	reference concentration at geometric center of enclosure	$y$	vertical coordinate
$C$	dimensionless species concentration = $(c - c_r)/\Delta c$	$Y$	dimensionless vertical coordinate = $y/W$
$D$	species diffusivity	<i>Greek symbols</i>	
$g$	gravitational acceleration	$\alpha$	thermal diffusivity
$H$	enclosure height	$\beta_T$	thermal expansion coefficient
$Ha$	Hartmann number = $B_o W \sqrt{\sigma/\mu}$	$\beta_c$	compositional expansion coefficient
$Le$	Lewis number = $\alpha/D$	$\Delta c$	characteristic concentration difference = $m^o W/D$
$m^o$	mass flux	$\Delta C_w$	wall-to-wall concentration difference = $C(0,0) - C(1,0)$
$N$	buoyancy ratio = $\beta_c m^o k / (\beta_T q' D)$	$\Delta T_w$	characteristic temperature difference = $q' W/k$
$Nu$	Nusselt number = $1/\Delta\theta_w$	$\Delta\theta$	wall-to-wall temperature difference = $\theta(0,0) - \theta(1,0)$
$p$	fluid pressure	$\phi$	dimensionless heat generation or absorption = $Q_o W^2 / (\rho c_p \alpha)$
$Pr$	Prandtl number = $\nu/\alpha$	$\mu$	dynamic viscosity
$q'$	heat flux	$\nu$	kinematic viscosity = $\mu/\rho$
$Q_o$	dimensional heat generation or absorption coefficient	$\theta$	dimensionless temperature = $(T - T_r)/\Delta T$
$Ra_T$	Rayleigh number = $g\beta_T q' W^5 / (k\alpha\nu)$	$\rho$	density
$Sh$	Sherwood number = $1/\Delta C_w$	$\rho^*$	dimensionless density = $NC - \theta$
$t$	time	$\sigma$	electrical conductivity
$T$	temperature	$\tau$	dimensionless time = $\alpha t/W^2$
$T_r$	reference temperature at geometric center of enclosure	$\tau_0$	period of oscillation
$u$	horizontal velocity component	$\Omega$	vorticity
$U$	dimensionless horizontal velocity component = $uW/\alpha$	$\Psi$	dimensionless stream function = $\psi/\alpha$
$v$	vertical velocity component	$\psi$	stream function
$V$	dimensionless vertical velocity component = $vW/\alpha$	$\zeta$	dimensionless vorticity = $\Omega W^2/\alpha$
		$\nabla^2$	Laplacian operator

heat flux in the presence of a transverse magnetic field. The effect of a magnetic field on free or natural convection in a rectangular enclosure having isothermal and adiabatic walls were also studied by Garandet et al. [11], Rudraiah et al. [25] and Al-Najem et al. [4].

Natural convection heat transfer induced by internal heat generation has recently received considerable attention because of numerous applications in geophysics and energy-related engineering problems. Such applications include heat removal from nuclear fuel debris, underground disposal of radioactive waste materials, storage of food-stuff, and exothermic chemical reactions in packed-bed reactor (see, for instance, [13]). Acharya and Goldstein [1] studied numerically two-dimensional natural convection of air in an externally heated vertical or inclined square box containing uniformly distributed internal energy sources. Recently, Churbanov et al. [10] studied numerically unsteady natural convection of a heat generating fluid in a vertical rectangular enclosure with isothermal or adiabatic

rigid walls. Other related works dealing with temperature-dependent heat generation effects can be found in the papers by Vajravelu and Nayfeh [29], Chamkha [9], Khanafer and Chamkha [15].

The problem of unsteady, laminar, hydromagnetic, double-diffusive natural convection flow inside a rectangular enclosure in the presence of heat generation or absorption has not been considered in the open literature. Because this situation is of fundamental interest and because it can have various possible applications such as crystal growth, geothermal reservoirs, nuclear fuel debris removal and solidification of metal alloys, it is of special interest to consider it in the present work. The top and bottom walls of the enclosure are assumed adiabatic and impermeable to mass transfer while the vertical walls are maintained at constant heat and mass fluxes. The magnetic Reynolds number is assumed small so that the induced magnetic field will be negligible.

**2. Mathematical formulation**

Consider unsteady, laminar, hydromagnetic, double-diffusive natural convection flow inside a rectangular enclosure in the presence of heat generation or absorption. The schematic of the problem is shown in Fig. 1. Uniform heat and mass fluxes  $q'$  and  $m^o$  are imposed along the left and right walls while the top and bottom walls are assumed adiabatic and impermeable to mass transfer. The enclosure is filled with an electrically conducting and heat generating or absorbing binary gas mixture. A magnetic field with uniform strength  $B_o$  is applied in the  $x$ -direction normal to the left and right walls. The fluid is assumed to be incompressible, viscous, and Newtonian. Both the viscous dissipation and Joule heating are assumed to be negligible. The magnetic Reynolds number is assumed to be small so that the induced magnetic field is neglected. No electric field is assumed to exist and the MHD Hall effect is negligible.

The governing equations for this investigation are based on the two-dimensional balance laws of mass, linear momentum, thermal energy, and concentration modified to include the magnetic field and heat generation or absorption effects. Taking into account the previous assumptions along with Boussinesq approximation with opposite thermal and compositional buoyancy forces, these equations can be written in dimensional form as

$$\frac{\partial u}{\partial x} + \frac{\partial v}{\partial y} = 0 \tag{1}$$

$$\frac{\partial u}{\partial t} + u \frac{\partial u}{\partial x} + v \frac{\partial u}{\partial y} = -\frac{1}{\rho} \frac{\partial p}{\partial x} + \nu \left( \frac{\partial^2 u}{\partial x^2} + \frac{\partial^2 u}{\partial y^2} \right) \tag{2}$$

$$\begin{aligned} \frac{\partial v}{\partial t} + u \frac{\partial v}{\partial x} + v \frac{\partial v}{\partial y} &= -\frac{1}{\rho} \frac{\partial p}{\partial y} + \nu \left( \frac{\partial^2 v}{\partial x^2} + \frac{\partial^2 v}{\partial y^2} \right) \\ &\quad - g\beta_T(T - T_r) + g\beta_c(c - c_r) - \frac{\sigma B_o^2}{\rho} v \end{aligned} \tag{3}$$

$$\frac{\partial T}{\partial t} + u \frac{\partial T}{\partial x} + v \frac{\partial T}{\partial y} = \alpha \left( \frac{\partial^2 T}{\partial x^2} + \frac{\partial^2 T}{\partial y^2} \right) + \frac{Q_o}{\rho c_p} (T - T_r) \tag{4}$$

$$\frac{\partial c}{\partial t} + u \frac{\partial c}{\partial x} + v \frac{\partial c}{\partial y} = D \left( \frac{\partial^2 c}{\partial x^2} + \frac{\partial^2 c}{\partial y^2} \right) \tag{5}$$

where  $x$ ,  $y$  and  $t$  are the horizontal and vertical distances and time, respectively.  $u$ ,  $v$ ,  $p$ ,  $T$  and  $c$  are the velocity components in the  $x$ - and  $y$ -direction, pressure, temperature and concentration, respectively.  $\beta_T$  and  $\beta_c$  are the thermal and compositional expansion coefficients, respectively.  $\rho$ ,  $\nu$ ,  $\alpha$ ,  $c_p$  and  $D$  are the fluid density, kinematic viscosity, thermal diffusivity, specific heat at constant pressure and the species diffusivity, respectively.  $g$ ,  $\sigma$ ,  $B_o$ ,  $Q_o$  are the gravitational acceleration, electrical conductivity, magnetic induction, and the dimensional heat generation or absorption coefficient, respectively.  $T_r$  and  $c_r$  are the reference temperature and concentration of the geometric center of the enclosure.

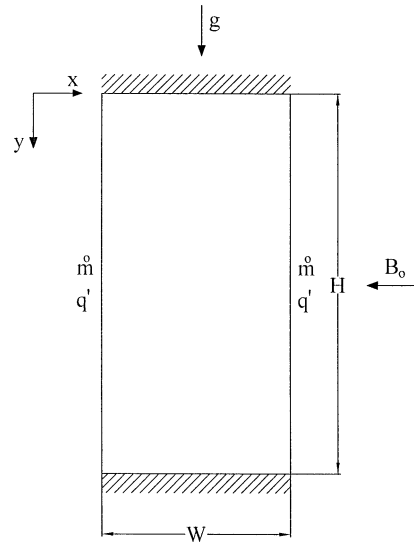


Fig. 1. Schematic diagram of the enclosure.

The boundary conditions for the problem can be written as

$$\begin{aligned} x = x, y = 0: & \quad u = 0, \quad v = 0, \quad \frac{\partial T}{\partial y} = 0, \quad \frac{\partial c}{\partial y} = 0 \\ x = x, y = H: & \quad u = 0, \quad v = 0, \quad \frac{\partial T}{\partial y} = 0, \quad \frac{\partial c}{\partial y} = 0 \\ x = 0, y = y: & \quad u = 0, \quad v = 0, \quad -k \frac{\partial T}{\partial x} = q', \quad -D \frac{\partial T}{\partial x} = m^o \\ x = W, y = y: & \quad u = 0, \quad v = 0, \quad -k \frac{\partial T}{\partial x} = q', \quad -D \frac{\partial T}{\partial x} = m^o \end{aligned} \tag{6}$$

where  $H$  and  $W$  are the height and the width of the enclosure, respectively.

The stream function and the vorticity can be defined in the usual way as

$$u = \frac{\partial \Psi}{\partial y}, \quad v = -\frac{\partial \Psi}{\partial x}, \quad \Omega = -\left( \frac{\partial^2 \Psi}{\partial x^2} + \frac{\partial^2 \Psi}{\partial y^2} \right) \tag{7}$$

where  $\Psi$  is the dimensional stream function and  $\Omega$  is the dimensional vorticity.

Eqs. (1) through (7) can be reduced (after eliminating the pressure gradient terms) and made dimensionless by using the following variables:

$$\begin{aligned} X = \frac{x}{W}, \quad Y = \frac{y}{W}, \quad \tau = \frac{\alpha t}{W^2} \\ \zeta = \frac{\Omega W^2}{\alpha}, \quad \psi = \frac{\Psi}{\alpha}, \quad \theta = \frac{(T - T_r) \Delta T}{\Delta T} \\ C = \frac{(c - c_r) \Delta c}{\Delta c}, \quad \Delta T = \frac{q' W}{k}, \quad \Delta c = \frac{m^o W}{D} \end{aligned} \tag{8}$$

to result the following dimensionless equations:

$$\zeta = \frac{\partial V}{\partial X} - \frac{\partial U}{\partial Y} = -\nabla^2 \psi \tag{9}$$

$$\frac{\partial \zeta}{\partial \tau} + U \frac{\partial \zeta}{\partial X} + V \frac{\partial \zeta}{\partial Y} = Pr \nabla^2 \zeta - Ra_T Pr \left( \frac{\partial \theta}{\partial X} - N \frac{\partial C}{\partial X} \right) - Ha^2 Pr \frac{\partial V}{\partial X} \quad (10)$$

$$\frac{\partial \theta}{\partial \tau} + U \frac{\partial \theta}{\partial X} + V \frac{\partial \theta}{\partial Y} = \nabla^2 \theta + \phi \theta \quad (11)$$

$$\frac{\partial C}{\partial \tau} + U \frac{\partial C}{\partial X} + V \frac{\partial C}{\partial Y} = \nabla^2 C / Le \quad (12)$$

where

$$Ha = B_o W \sqrt{\frac{\sigma}{\mu}}, \quad N = \frac{\beta_c m^o / D}{\beta_T q' / k} \\ Ra_T = \frac{g \beta_T q' W^4}{k \alpha \nu}, \quad Pr = \nu / \alpha \quad (13) \\ Le = \frac{\alpha}{D}, \quad \phi = \frac{Q_o W^2}{\rho c_p \alpha}$$

are the Hartmann number, buoyancy ratio, thermal Rayleigh number, Prandtl number, Lewis number and the dimensionless heat generation or absorption coefficient, respectively.

The dimensionless boundary conditions become

$Y = 0$  (top horizontal wall):

$$U = V = \psi = 0, \quad \zeta = - \left( \frac{\partial^2 \psi}{\partial Y^2} \right), \quad \frac{\partial \theta}{\partial Y} = 0 \\ \frac{\partial C}{\partial Y} = 0 \quad (14a)$$

$Y = H/W$  (bottom horizontal wall):

$$U = V = \psi = 0, \quad \zeta = - \left( \frac{\partial^2 \psi}{\partial Y^2} \right), \quad \frac{\partial \theta}{\partial Y} = 0 \\ \frac{\partial C}{\partial Y} = 0 \quad (14b)$$

$X = 0$  (left vertical wall):

$$U = V = \psi = 0, \quad \zeta = - \left( \frac{\partial^2 \psi}{\partial X^2} \right), \quad \frac{\partial \theta}{\partial X} = -1 \\ \frac{\partial C}{\partial X} = -1 \quad (14c)$$

$X = 1$  (right vertical wall):

$$U = V = \psi = 0, \quad \zeta = - \left( \frac{\partial^2 \psi}{\partial X^2} \right), \quad \frac{\partial \theta}{\partial X} = -1 \\ \frac{\partial C}{\partial X} = -1 \quad (14d)$$

### 3. Numerical method

The numerical algorithm used to solve Eqs. (9) through (12) subject to Eqs. (14) was based on the finite-difference methodology. The time derivatives are replaced by two-point backward difference formulae and central differencing is employed to approximate the spatial derivatives. The obtained discretized equations are then solved iteratively using a line-by-line application of the Thomas algorithm. The numerical procedure starts with calculating the concentration,

temperature, vorticity and then the stream function. The velocity components are then evaluated at the desired location within the enclosure. This method was stable and gave results that are very close to the numerical results obtained by Nishimura et al. [20] using the finite-element method for the case of isothermal vertical walls.

The numerical computations were performed on a high-speed alpha machine. In all the results obtained, an aspect ratio  $AR = 2$  was used for the rectangular enclosure. A computational domain consisting of  $31 \times 41$  grid points with uniform grid spacing in both the  $x$ - and  $y$ -directions was found to be sufficient for producing accurate results. A time step of  $10^{-5}$  was used through out the calculations. The convergence criterion required that the difference between the current and previous iterations for all of the dependent variables be  $10^{-4}$ .

The Nusselt and Sherwood numbers are averaged and evaluated along the left boundary of the enclosure which may be expressed as

$$\overline{Nu} = - \int_0^2 \left( \frac{\partial \theta}{\partial X} \right) dY \quad (15)$$

$$\overline{Sh} = - \int_0^2 \left( \frac{\partial C}{\partial X} \right) dY \quad (16)$$

### 4. Grid convergence and validation

In order to check on the accuracy of the numerical technique employed for the solution of the problem considered in the present study, it was validated by performing simulation for double-diffusive convection flow in a vertical rectangular enclosure with combined horizontal temperature and concentration gradients and in the absence of the magnetic field and the heat generation or absorption effects which was reported earlier by Nishimura et al. [20]. Fig. 2 presents a graphical comparison of the contour maps of the streamlines, temperature, concentration and density for a buoyancy ratio of 0.8 of the present work and those reported earlier by Nishimura et al. [20]. It is clear from this figure that good agreement between the results exists. In addition, Table 1 shows a favorable quantitative comparison of the stream function extrema  $|\psi_{\max}|$  and  $|\psi_{\min}|$  at  $N = 1$  obtained by three different numerical methods and reported by Morega and Nishimura [18], Nishimura et al. [20] and the present work for a period of oscillation  $\tau_0$ . These comparisons lend confidence in the accuracy of the numerical procedure employed in the present work.

The effects of the grid size on the  $x$ -component of velocity  $U$  and temperature  $\theta$  profiles at the enclosure mid-section were studied. Three different grid sizes were used. These were  $16 \times 21$ ,  $31 \times 41$  and  $61 \times 81$ . It was observed that the profiles of  $U$  and  $\theta$  changed slightly with these grid sizes and that the  $31 \times 41$  grids solution is almost the same as that of the  $61 \times 81$  grids. For this reason, a computational

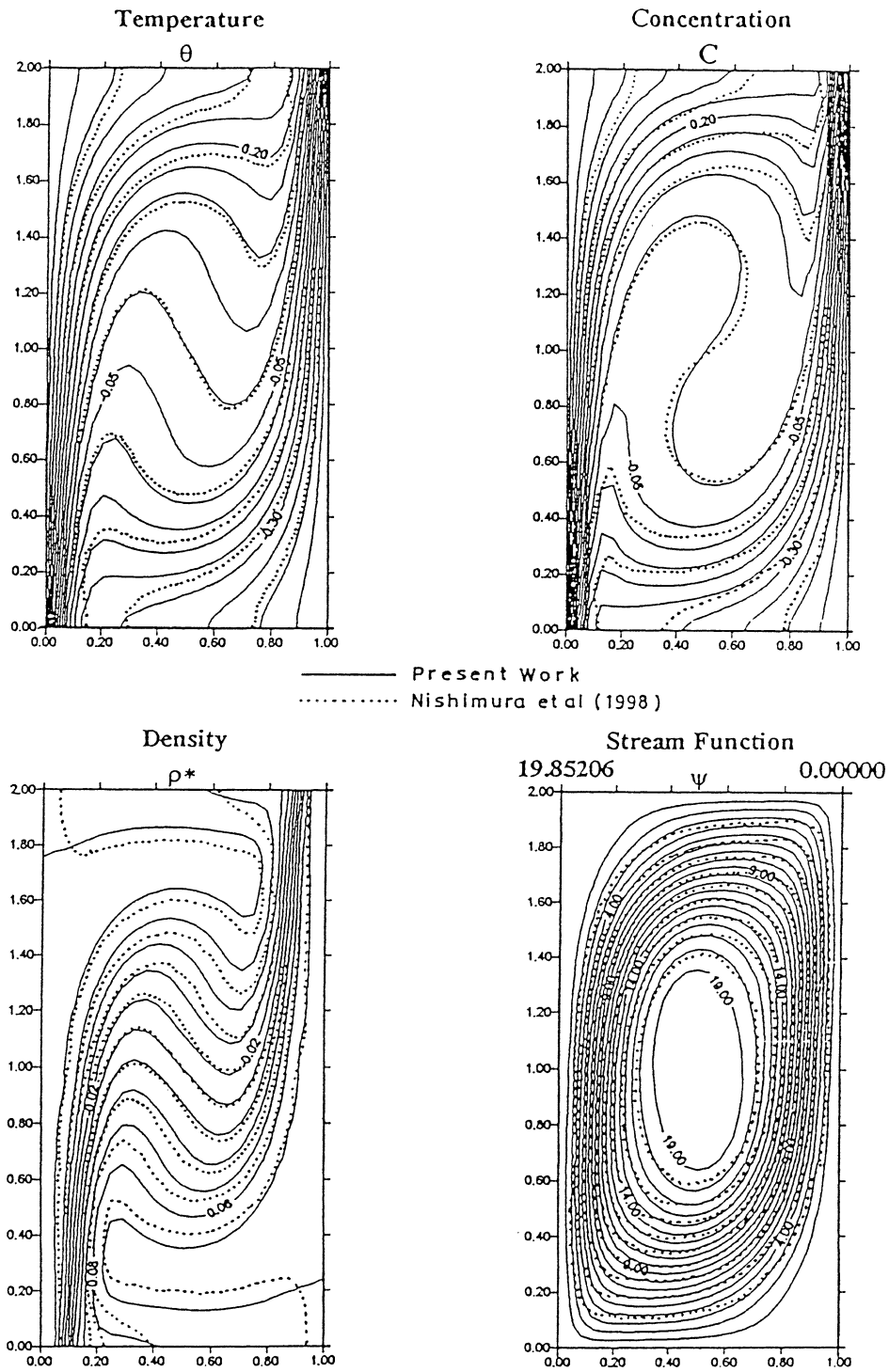


Fig. 2. Comparison of present work with Nishimura et al. [20] for  $Ha = 0$ ,  $Le = 2.0$ ,  $N = 0.8$ ,  $Pr = 1.0$ ,  $Ra_T = 10^5$  and  $\phi = 0$ .

domain consisting of  $31 \times 41$  grid points was employed for all of the results to be reported in the present work.

**5. Results and discussion**

In this section, representative numerical results for the streamline, temperature, and concentration contours as well

as selected velocity, temperature and concentration profiles at mid-section of the enclosure for various values of Hartmann number  $Ha$  and the heat generation or absorption coefficient  $\phi$  will be reported. In addition, representative results for the average Nusselt number  $\overline{Nu}$  and the average Sherwood number  $\overline{Sh}$  for various physical conditions will be presented and discussed.

Table 1

Comparison of present work with those of Morega and Nishimura [18] and Nishimura et al. [20] for  $N = 1.0$ 

Parameter	Spectral method Morega and Nishimura [18]	Finite-element method Nishimura et al. [20]	Finite-difference method Present work
$\tau_0$	0.0494	0.0497	0.0509
$\max \psi_{\max} $	26.8	26.7	27.8
$\min \psi_{\max} $	12.7	12.9	13.7
$\max \psi_{\min} $	5.52	5.76	5.85
$\min \psi_{\min} $	0.333	0.351	0.333

Fig. 3 presents steady-state contour maps for the streamline, temperature, and concentration for various values of the Hartmann number  $Ha$  for  $Le = 2.0$ ,  $N = 1.0$ ,  $Pr = 1.0$ ,  $Ra_T = 10^5$  and  $\phi = 0$ . The condition  $N = 1.0$  indicates that the flow is dominated by equal but opposing effects of both thermal and compositional buoyancies. When  $N < 1.0$ , the flow is primarily dominated by thermal buoyancy effects whereas for  $N > 1.0$  the flow is mainly dominated by compositional buoyancy effects. In the absence of the magnetic field ( $Ha = 0$ ), the flow is characterized by a primary recirculating eddy of relatively high velocity circulating around the entire enclosure and centered in its core region. Because of the boundary-layer effects, both the temperature and concentration fields are characterized by sharp drops in their values near the vertical walls of the enclosure. Also, the temperature and concentration contour maps are not horizontally uniform in the core region of the enclosure. The application of a transverse magnetic field has the tendency to slow down the movement of the fluid in the enclosure. As a result, the primary recirculating eddy tends to be stretched or elongated in the vertical direction. This process continues as the strength of the magnetic field increases until the flow separates forming two smaller and slower recirculating eddies positioned close to each of the insulated walls of the enclosure. The retardation effect of the magnetic effect is observed from the maximum intensity of circulation  $\psi_{\max}$ . The value of  $\psi_{\max}$  for  $Ha = 0$  is 7.4445 while it is equal to 6.3937, 5.1369, 4.2013 and 3.0384 for  $Ha = 5.0, 10, 15$  and  $25$ , respectively. The temperature and concentration contour maps tend to become more horizontally uniform in the core region of the enclosure as  $Ha$  increases indicating the approach to a quasi-conduction regime. In addition to the flow retardation effect, the magnetic field is seen to suppress the overall heat transfer in the enclosure. This suppression of convective flows by the use of magnetic fields has proven to be effective in controlling melts and has now been widely practiced in the metals semiconductor crystal growth industries (see [26]).

Figs. 4–7 present typical profiles for the horizontal and vertical velocities, temperature and concentration at mid-section of the enclosure for various values of the Hartmann number  $Ha$ , respectively. These profiles show an anti-symmetric trend about the mid horizontal direction of the enclosure. It is predicted that, in the region close to the left vertical wall of the enclosure, the horizontal velocity decreases while all of the vertical velocity, temperature, and

concentration increase due to increases in the Hartmann number. The opposite effect is observed in the region close to the right vertical wall of the enclosure. The magnitude of the net velocity tends to decrease as the strength of the magnetic field increases. The left vertical wall temperature and concentration tend to increase as the Hartmann number increases. This produces lower left vertical wall heat and mass transfer coefficients. The influence of the magnetic field is seen to be more pronounced on the temperature profiles than on the concentration profiles.

In Fig. 8, it is observed that for  $N = 1.0$  the presence of a heat sink (absorption,  $\phi < 0$ ) within the enclosure causes higher heat transfer rates with the thermal recirculation within the enclosure being less stretched and more centered. However, the presence of a heat source (generation,  $\phi > 0$ ) produces less heat transfer rates and the thermal recirculation tends to stretch and then separate into two vortices, one close to each of the bottom and top walls of the enclosure. The temperature and concentration contours in the core region of the enclosure tend to become more horizontally uniform as the heat generation effect is increased.

Figs. 9–12 depict the influence of  $\phi$  on the profiles of  $U$ ,  $V$ ,  $\theta$  and  $C$  at the enclosure mid-section for  $N = 1.0$ , respectively. It is clearly observed that in the vicinity of the left vertical wall, heat generation reduces the  $x$ -component of velocity while it increases all of the  $y$ -component of velocity, temperature and concentration. The opposite effect is predicted due the presence of a heat sink. In addition, the right vertical wall temperature and concentration tend to decrease as  $\phi$  increases. The effect of heat generation on the temperature profiles is predicted to be more than that associated with the heat absorption case for the same parametric values.

The effects of the Hartmann number  $Ha$  and the heat generation or absorption coefficient  $\phi$  on the average Nusselt number  $\overline{Nu}$  and the average Sherwood number  $\overline{Sh}$  for a buoyancy ratio of  $N = 1.0$  are presented in Tables 2 and 3, respectively. As discussed before, it is observed that both of  $\overline{Nu}$  and  $\overline{Sh}$  have a decreasing trend with increasing values of  $Ha$ . In addition, it is observed that heat generation ( $\phi > 0$ ) decreases both the average Nusselt and Sherwood numbers while heat absorption ( $\phi < 0$ ) increases them. These behaviors are related to the left vertical wall temperature and concentration. When they increase, both of  $\overline{Nu}$  and  $\overline{Sh}$  tend to decrease. On the other hand, when they decrease both of  $\overline{Nu}$  and  $\overline{Sh}$  tend to increase.

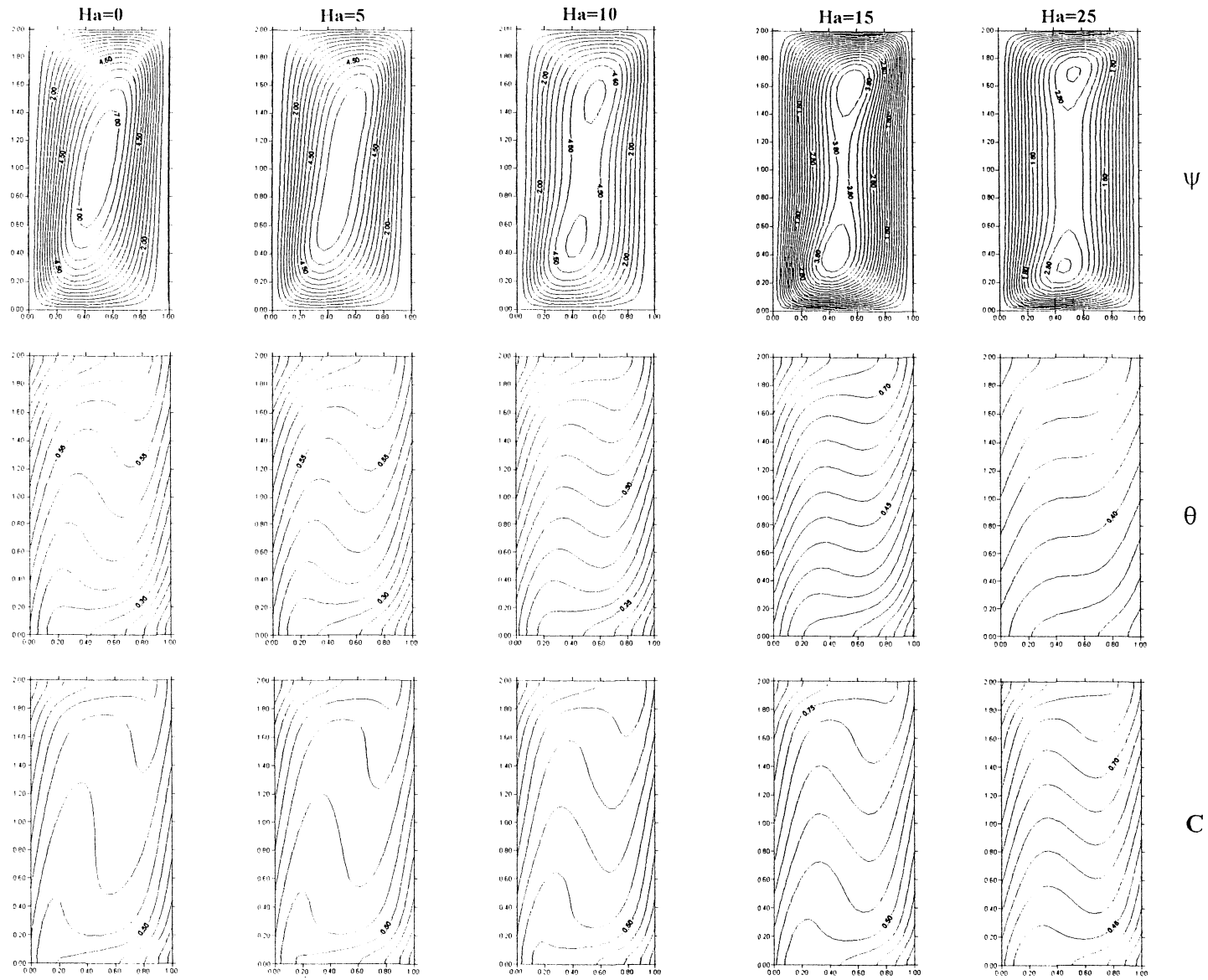


Fig. 3. Effect of  $Ha$  on the contours of streamlines, temperature and concentration for  $Le = 2.0$ ,  $N = 1.0$ ,  $Pr = 1.0$ ,  $Ra_T = 10^5$  and  $\phi = 0$ .

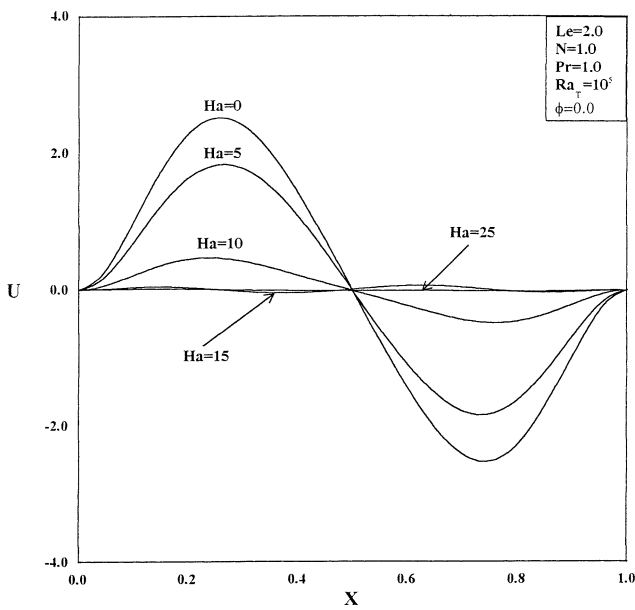


Fig. 4. Effect of  $Ha$  on  $x$ -component velocity profiles at enclosure mid-section.

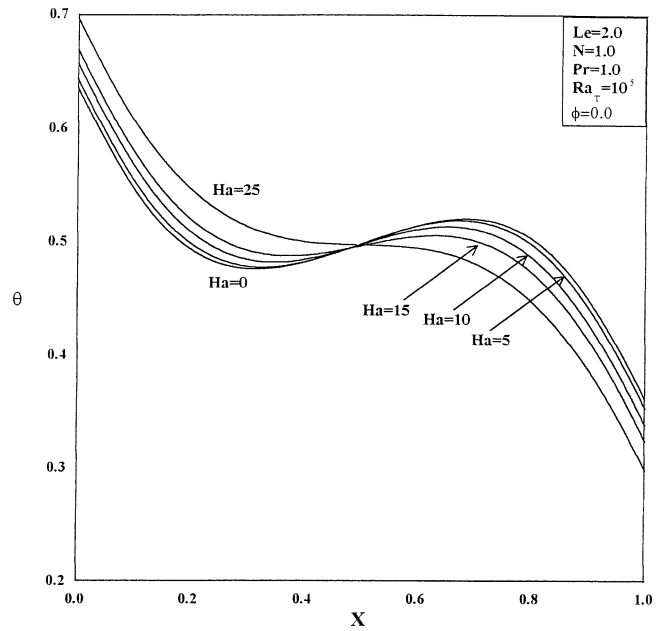


Fig. 6. Effect of  $Ha$  on temperature profiles at enclosure mid-section.

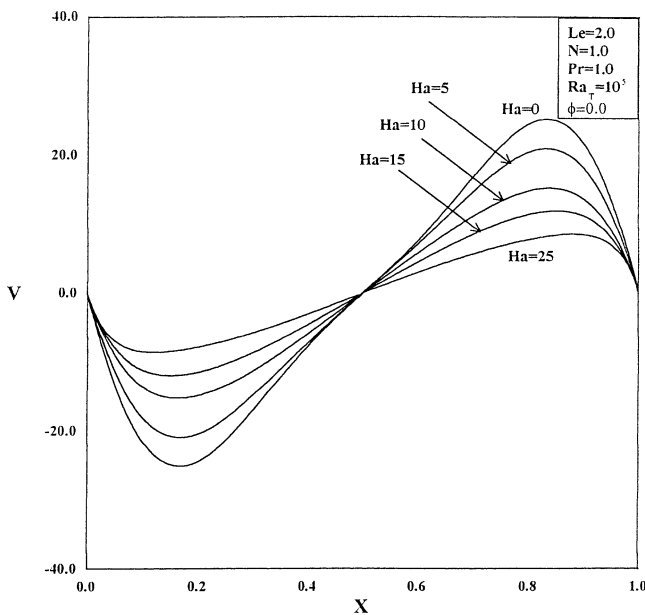


Fig. 5. Effect of  $Ha$  on  $y$ -component velocity profiles at enclosure mid-section.

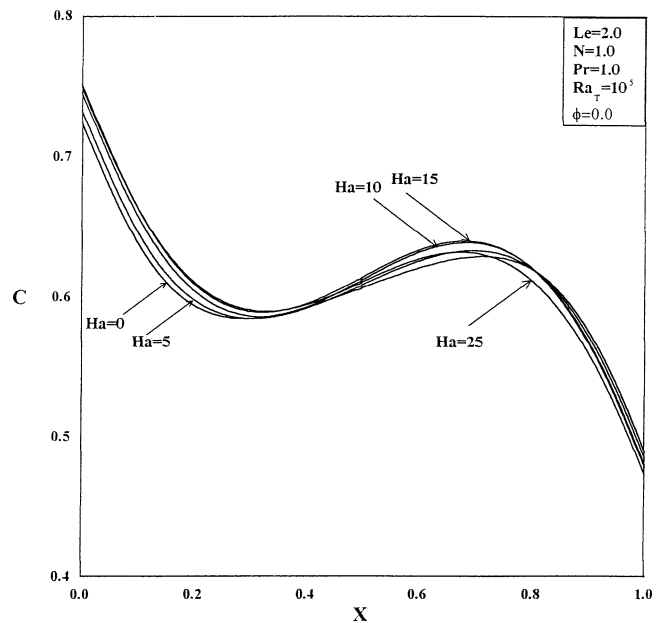


Fig. 7. Effect of  $Ha$  on concentration at enclosure mid-section.

Figs. 13–18 illustrate the influence of the buoyancy ratio  $N$  and the Rayleigh number  $Ra$  on the average Nusselt and Sherwood numbers  $\overline{Nu}$  and  $\overline{Sh}$  for three different values of the Lewis number  $Le$ , respectively. It is predicted that both  $\overline{Nu}$  and  $\overline{Sh}$  increase as the Rayleigh number increases for most of the values of  $N$  considered. In addition, it is interesting to observe from these figures the existence of minimum values in  $\overline{Nu}$  and  $\overline{Sh}$  for a critical buoyancy ratio  $N_{cr}$ . The value of  $N_{cr}$  changes depending on the value of  $Le$ . For example, for  $Le = 1.0$ , the value of  $N_{cr}$  is unity.

For a specific value of  $Le$ , both  $\overline{Nu}$  and  $\overline{Sh}$  tend to decrease with increasing values of  $N$  for  $N < N_{cr}$  and to increase with increasing values of  $N$  for  $N > N_{cr}$ . For  $Le = 1.0$ , the profiles of  $\overline{Nu}$  and  $\overline{Sh}$  with  $N$  are symmetric about the value  $N_{cr} = 1.0$  for all values of  $Ra$  considered. However, for  $Le = 0.1$ , the critical value of  $N$  occurs around  $N = 0.5$  while for  $Le = 10$  it occurs at a value of  $N > 2$  as is obvious from the trend of the curves for this case. No symmetry about  $N_{cr}$  appears to exist in the range of  $N$  between 0 and 2.0. It is possible that this may not be the case if the range

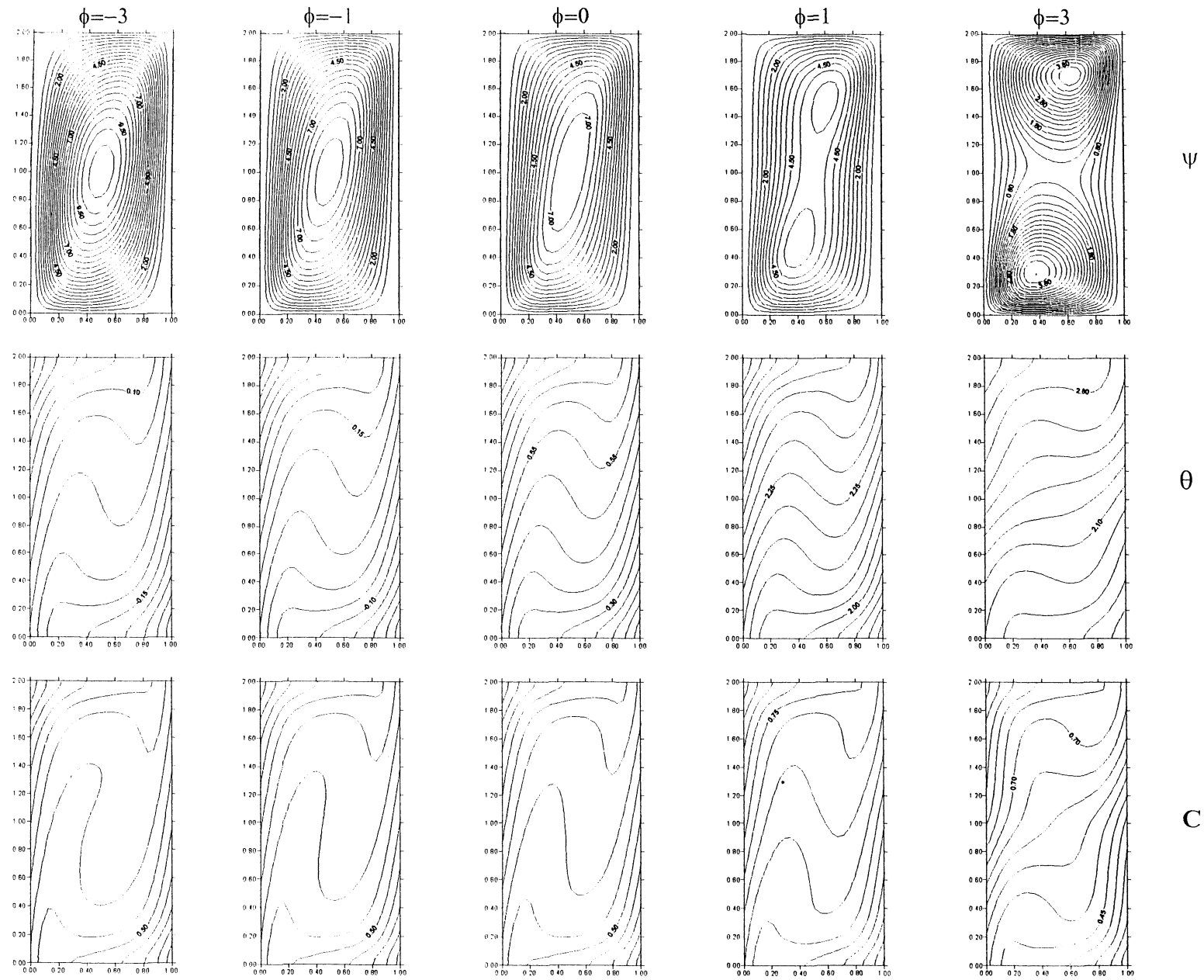


Fig. 8. Effect of  $\phi$  on the contours of stream lines, temperature and concentration for  $Ha = 0$ ,  $Le = 2.0$ ,  $N = 1.0$ ,  $Pr = 1.0$  and  $Ra_T = 10^5$ .

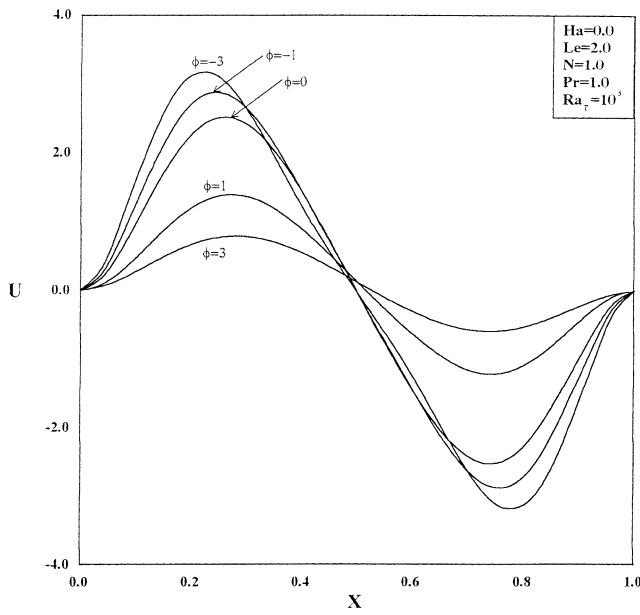


Fig. 9. Effect of  $\phi$  on  $x$ -component velocity profiles at enclosure mid-section.

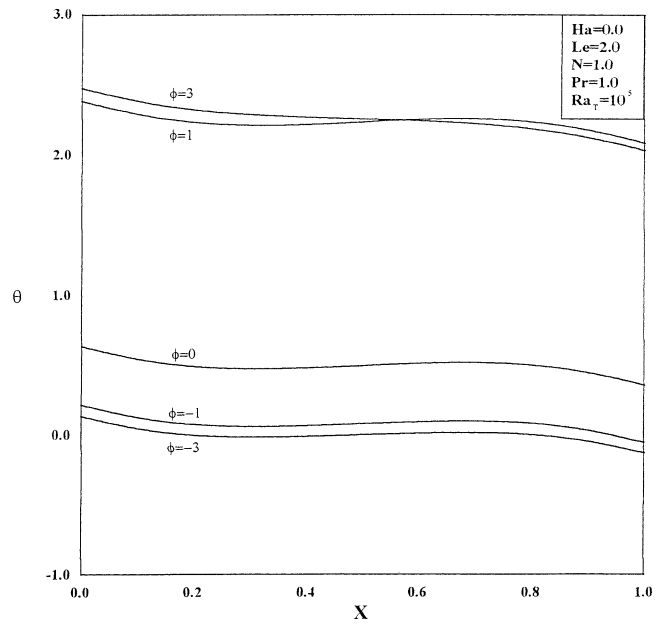


Fig. 11. Effect of  $\phi$  on temperature profiles at enclosure mid-section.

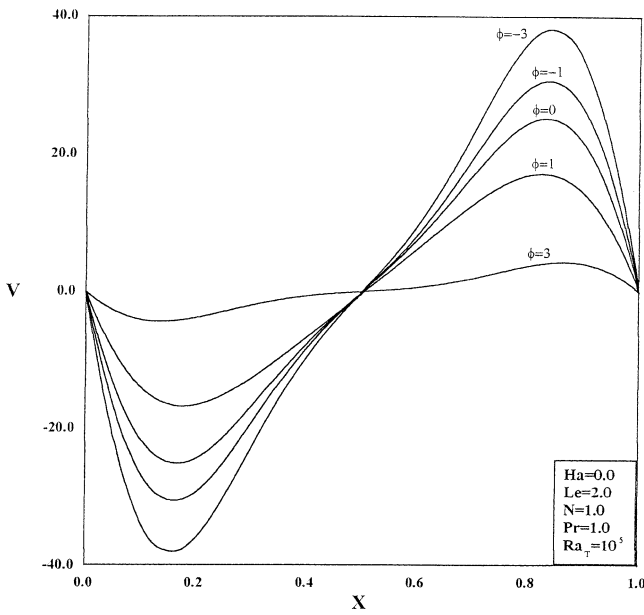


Fig. 10. Effect of  $\phi$  on  $y$ -component velocity profiles at enclosure mid-section.

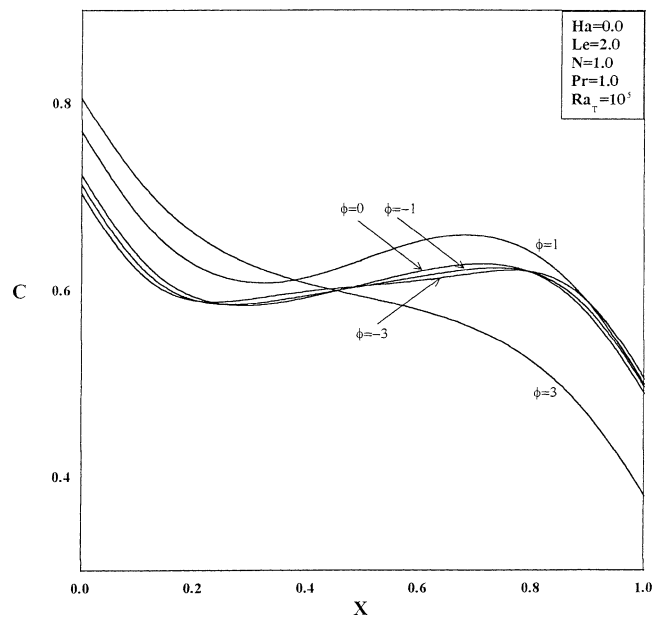


Fig. 12. Effect of  $\phi$  on concentration profiles at enclosure mid-section.

of  $N$  is expanded below  $N = 0$  for  $Le = 0.1$  and above  $N = 2.0$  for  $Le = 10$ . Furthermore, it is observed that the values of  $\overline{Nu}$  increase as  $Le$  increases for most values of  $N$  while the values of  $\overline{Sh}$  increase as  $Le$  increases for all values of  $N$ . The physical behaviors illustrated in these figures are associated with the thermal-dominated and compositional-dominated regimes discussed earlier and similar trends have been reported in the open literature (see, for example, [8,19, 27]).

Table 2  
Effects of  $Ha$  on the average Nusselt and Sherwood numbers for  $Le = 2.0$ ,  $Pr = 1.0$ ,  $N = 1.0$ ,  $Ra_T = 10^5$  and  $\phi = 0$

Parameter	$\overline{Nu}$	$\overline{Sh}$
$Ha = 0.0$	3.319	4.030
$Ha = 5.0$	3.215	3.909
$Ha = 10$	3.048	3.797
$Ha = 15$	2.868	3.744
$Ha = 25$	2.497	3.652

Table 3  
Effects of  $\phi$  on the average Nusselt and Sherwood numbers for  $Ha = 0.0$ ,  $Le = 2.0$ ,  $Pr = 1.0$ ,  $N = 1.0$ , and  $Ra_T = 10^5$

Parameter	$\overline{Nu}$	$\overline{Sh}$
$\phi = -3.0$	3.354	4.408
$\phi = -1.0$	3.345	4.210
$\phi = 0.0$	3.319	4.030
$\phi = 1.0$	3.239	3.758
$\phi = 3.0$	2.769	3.043

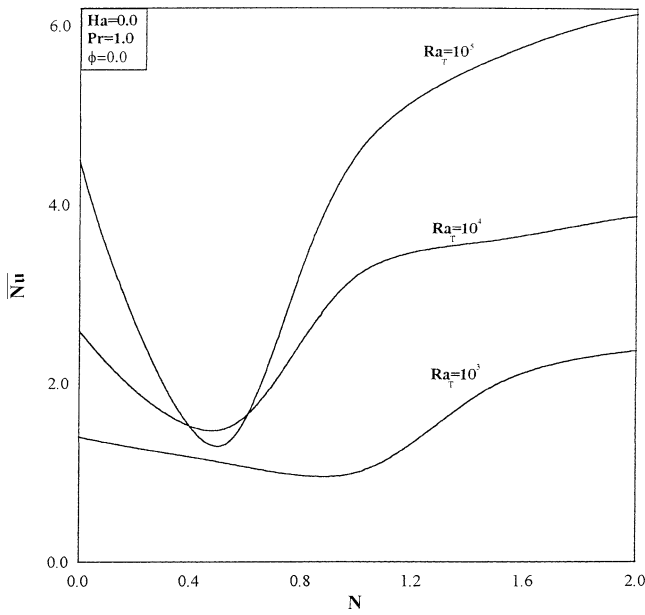


Fig. 13. Effect of  $Ra_T$  and  $N$  on average Nusselt number for  $Le = 0.1$ .

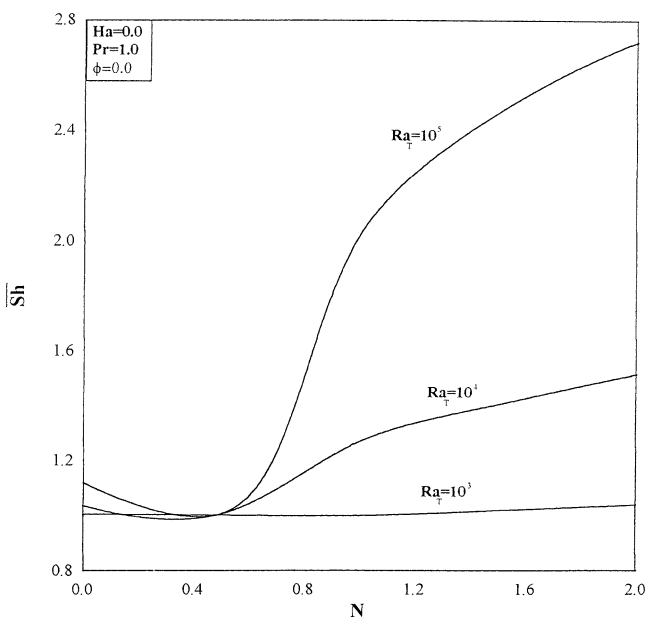


Fig. 14. Effect of  $Ra_T$  and  $N$  on average Sherwood number for  $Le = 0.1$ .

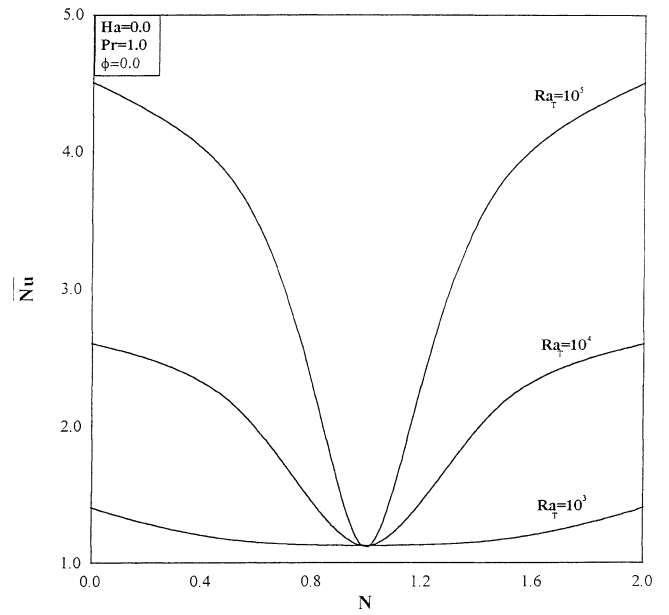


Fig. 15. Effect of  $Ra_T$  and  $N$  on average Nusselt number for  $Le = 1.0$ .

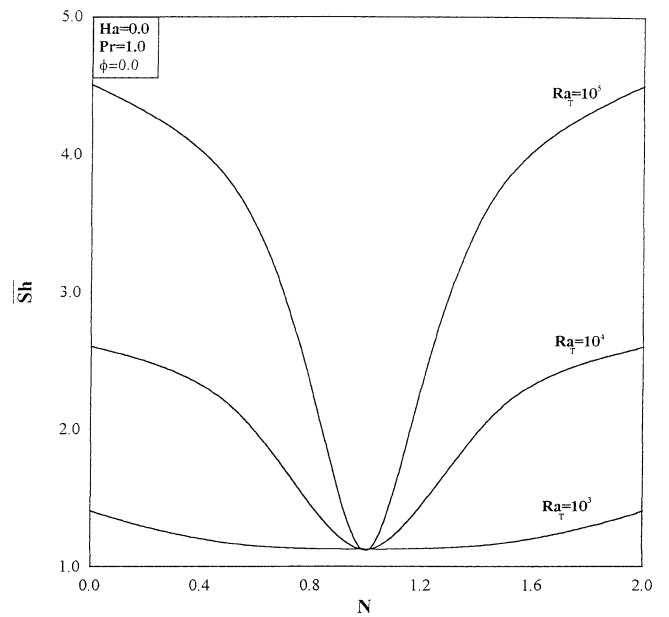


Fig. 16. Effect of  $Ra_T$  and  $N$  on average Sherwood number for  $Le = 1.0$ .

### 6. Conclusions

The application of external magnetic fields to control the behavior of the melts during solidification processes including casting and crystal growth is widespread in the metals and semiconductor industries. These applications involve understanding of the characteristics of heat and mass transfer phenomenon occurring in the melt. In this work, double-diffusive convection flow due to opposing temperature and concentration gradients of an electrically conducting and heat-generating or absorbing fluid inside a rectangular enclosure with uniform side heat and mass fluxes in the presence of a transverse magnetic field was

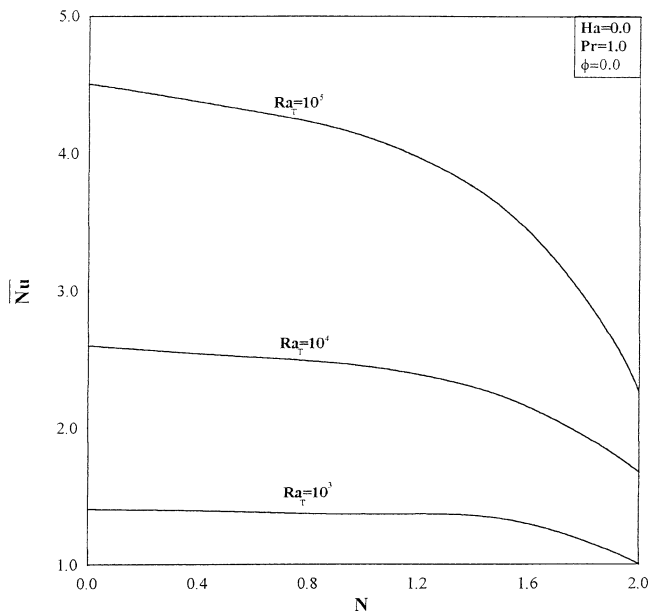


Fig. 17. Effect of  $Ra_T$  and  $N$  on average Nusselt number for  $Le = 10.0$ .

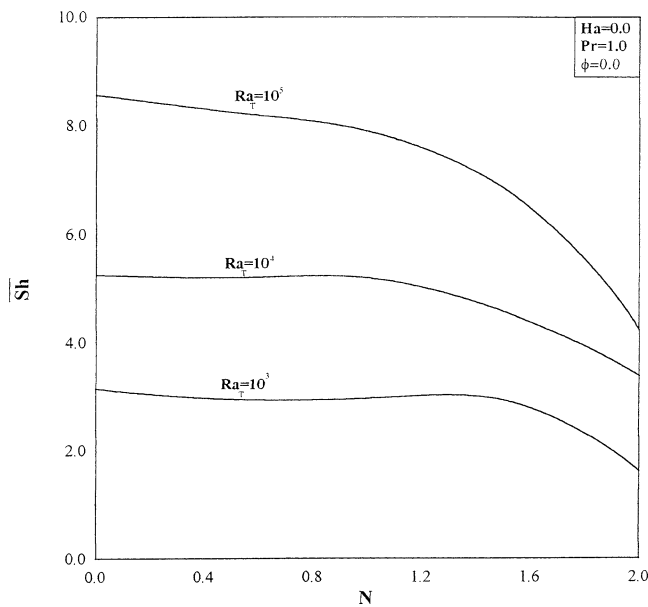


Fig. 18. Effect of  $Ra_T$  and  $N$  on average Sherwood number for  $Le = 10.0$ .

studied numerically. The line method based on the finite-difference technique was employed for the solution of the present problem. Comparisons with previously published work on special cases of the problem were performed and found to be in good agreement. Graphical results for various parametric conditions were presented and discussed. It was found that the heat and mass transfer mechanisms and the flow characteristics inside the enclosure depended strongly on the magnetic field and heat generation or absorption effects. The effect of the magnetic field was found to reduce the overall heat transfer and fluid circulation within the enclosure. In addition, it was predicted that both the average Nusselt and Sherwood numbers increased owing

the presence of heat absorption effects while they decreased when heat generation effects were present. Furthermore, as the Lewis number was increased, both the average Nusselt and Sherwood numbers were increased for most values of the buoyancy ratios considered. Distinctive minima in the values of both the average Nusselt and Sherwood numbers were predicted for specific values of the buoyancy ratio and the Lewis number.

## References

- [1] S. Acharya, R.J. Goldstein, Natural convection in an externally heated vertical or inclined square box containing internal energy sources, *ASME J. Heat Transfer* 107 (1985) 855–866.
- [2] F. Alavyoon, Y. Masuda, On natural convection in vertical porous enclosures due to opposing fluxes of heat and mass prescribed at the vertical walls, *Internat. J. Heat Mass Transfer* 37 (1994) 195–206.
- [3] S. Alchaar, P. Vasseur, E. Bilgen, Natural convection heat transfer in a rectangular enclosure with a transverse magnetic field, *ASME J. Heat Transfer* 117 (1995) 668–673.
- [4] N.M. Al-Najem, K.M. Khanafer, M.M. El-Refaei, Numerical study of laminar natural convection in tilted enclosure with transverse magnetic field, *Internat. J. Numer. Methods Heat Fluid Flow* 8 (1998) 651–672.
- [5] C. Beghein, F. Haghigat, F. Allard, Numerical study of double-diffusive natural convection in a square cavity, *Internat. J. Heat Mass Transfer* 35 (1992) 833–846.
- [6] A. Bejan, Mass and heat transfer by natural convection in a vertical cavity, *Internat. J. Heat Fluid Flow* 6 (1985) 149–159.
- [7] R. Bennacer, H. Beji, F. Oueslati, A. Belghith, Multiple natural convection solution in porous media under cross temperature and concentration gradients, *Numer. Heat Transfer, Part A* 39 (2001) 553–567.
- [8] P. Bera, V. Eswaran, P. Singh, Numerical study of heat and mass transfer in an anisotropic porous enclosure due to constant heating and cooling, *Numer. Heat Transfer, Part A* 34 (1998) 887–905.
- [9] A.J. Chamkha, Non-Darcy fully developed mixed convection in a porous medium channel with heat generation: Absorption and hydromagnetic effects, *Numer. Heat Transfer, Part A* 32 (1997) 653–675.
- [10] A.G. Churbanov, P.N. Vabishchevich, V.V. Chudanov, V.F. Strizhov, A numerical study on natural convection of a heat generating fluid in rectangular enclosures, *Internat. J. Heat Mass Transfer* 37 (1994) 2969–2984.
- [11] J.P. Garandet, T. Alboussiere, R. Moreau, Buoyancy driven convection in a rectangular enclosure with a transverse magnetic field, *Internat. J. Heat Mass Transfer* 35 (1992) 741–748.
- [12] J.M. Hyun, J.W. Lee, Double-diffusive convection in a rectangle with cooperating horizontal gradients of temperature and concentration gradients, *Internat. J. Heat Mass Transfer* 33 (1990) 1605–1617.
- [13] S. Kakac, W. Aung, R. Viskanta, *Natural Convection—Fundamentals and Applications*, Hemisphere, Washington, DC, 1985.
- [14] Y. Kamotani, L.W. Wang, S. Ostrach, H.D. Jiang, Experimental study of natural convection in shallow enclosures with horizontal temperature and concentration gradients, *Internat. J. Heat Mass Transfer* 28 (1985) 165–173.
- [15] K. Khanafer, A.J. Chamkha, Hydromagnetic natural convection from and inclined porous square enclosure with heat generation, *Numer. Heat Transfer, Part A* 33 (1998) 891–910.
- [16] J. Lee, M.T. Hyun, K.W. Kim, Natural convection in confined fluids with combined horizontal temperature and concentration gradients, *Internat. J. Heat Mass Transfer* 31 (1988) 1969–1977.
- [17] J.W. Lee, J.M. Hyun, Double-diffusive convection in a rectangle with opposing horizontal and concentration gradients, *Internat. J. Heat Mass Transfer* 33 (1990) 1619–1632.

- [18] A.M. Morega, T. Nishimura, Double-diffusive convection by Chebyshev collocation method, *Technol. Rep. Yamaguchi Univ.* 5 (1996) 259–276.
- [19] P. Nithiarasu, K.N. Seetharamu, T. Sundararajan, Double-diffusive natural convection in an enclosure filled with fluid-saturated porous medium: A generalized non-Darcy approach, *Numer. Heat Transfer, Part A* 30 (1996) 413–426.
- [20] T. Nishimura, M. Wakamatsu, A.M. Morega, Oscillatory double-diffusive convection in a rectangular enclosure with combined horizontal temperature and concentration gradients, *Internat. J. Heat Mass Transfer* 41 (1998) 1601–1611.
- [21] G.M. Oreper, J. Szekely, The effect of an externally imposed magnetic field on buoyancy driven flow in a rectangular cavity, *J. Cryst. Growth* 64 (1983) 505–515.
- [22] S. Ostrach, Natural convection with combined driving forces, *Phys. Chem. Hydrodyn.* 1 (1980) 233–247.
- [23] S. Ostrach, H.D. Jiang, Y. Kamotani, Thermo-solutal convection in shallow enclosures, in: *ASME–JSME Thermal Engineering Joint Conference*, Hawaii, 1987.
- [24] H. Ozoe, M. Maruo, Magnetic and gravitational natural convection of melted silicon—two dimensional numerical computations for the rate of heat transfer, *JSME* 30 (1987) 774–778.
- [25] N. Rudraiah, R.M. Barron, M. Venkatachalappa, C.K. Subbaraya, Effect of a magnetic field on free convection in a rectangular enclosure, *Internat. J. Engrg. Sci.* 33 (1995) 1075–1084.
- [26] R.W. Series, D.T.J. Hurler, The use of magnetic fields in semiconductor crystal growth, *J. Cryst. Growth* 133 (1991) 305–328.
- [27] O.V. Trevisan, A. Bejan, Mass and heat transfer by natural convection in a vertical slot filled with porous medium, *Internat. J. Heat Mass Transfer* 29 (1986) 403–415.
- [28] O.V. Trevisan, A. Bejan, Combined heat and mass transfer by natural convection in a vertical enclosure, *ASME J. Heat Transfer* 109 (1987) 104–112.
- [29] K. Vajravelu, J. Nayfeh, Hydromagnetic convection at a cone and a wedge, *Internat. Commun. Heat Mass Transfer* 19 (1992) 701–710.
- [30] R. Viskanta, T.L. Bergman, F.P. Incropera, Double-diffusive natural convection, in: S. Kakac, W. Aung, R. Viskanta (Eds.), *Natural Convection: Fundamentals and Applications*, Hemisphere, Washington, DC, 1985, pp. 1075–1099.